

New STIS Observations of the Transiting-Planet System HD 209458

David Charbonneau (California Institute of Technology, dc@caltech.edu), Timothy M. Brown (National Center for Atmospheric Research), Ronald L. Gilliland (Space Telescope Science Institute), & Robert W. Noyes (Harvard-Smithsonian Center for Astrophysics)

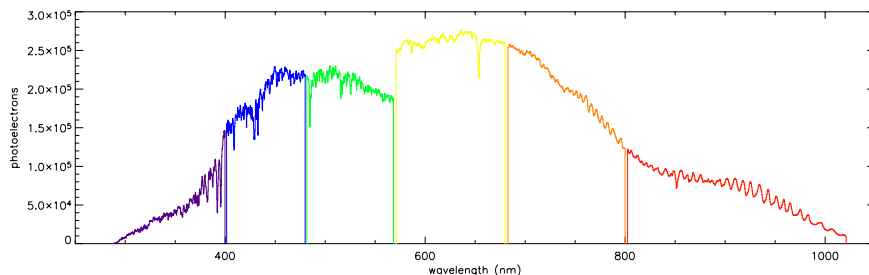
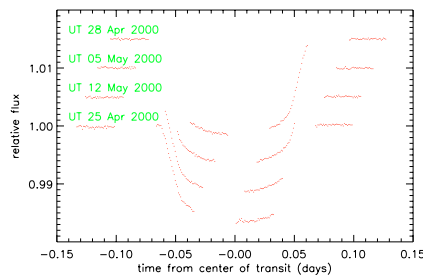
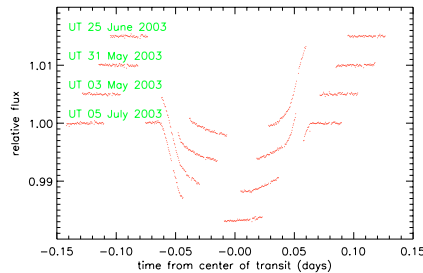
Summary of the Data and Orbit Determination Improvement

We have obtained 4 visits (of 5 HST-orbits each) of low-resolution spectra of the G0V star HD 209458 during times of transit by its planetary companion ($R_p = 1.35 R_{\text{Jup}}$, $M_p = 0.69 M_{\text{Jup}}$). We use the STIS spectrograph to disperse the light over many pixels, and then add up the recorded electrons to produce a photometric index over a desired bandpass. The data quality for the first orbit of each visit is generally compromised due to HST reaching equilibrium at the new pointing, but the other 4 orbits yield time series with a cadence of 40 seconds and a precision of better than 100 μmag .

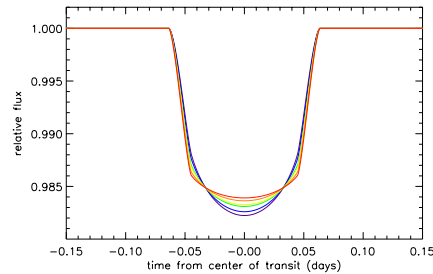
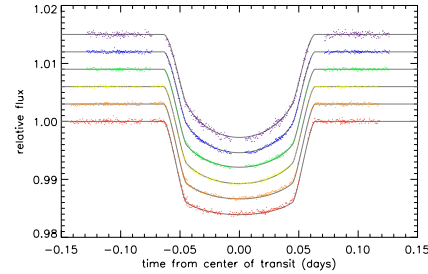
We are able to determine the times of center of transit with a typical precision of better than 10 s. Combining these new visits with similar STIS time series gathered in spring 2000 (see figure below), we are able to greatly improve the precision of our estimate of the orbital period:

Study	Period (days)	Uncertainty (days)
Charbonneau et al. (2000)	3.5250	0.003
Castellano et al. (2000)	3.524736	0.000045
Brown et al. (2001)	3.52480	0.00004
Robichon & Arenou (2000)	3.524739	0.000014
This poster	3.52474895	0.00000096

The uncertainty in the period estimate is now only 83 ms. It will now be possible to search for small offsets in the transit timing (manifesting as apparent changes in the orbital period) that might indicate additional masses in the HD209458 system.



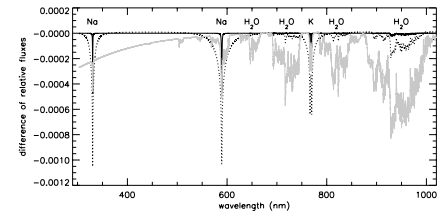
Limb-Darkened Light Curves



The planet acts a probe of the stellar limb-darkening, allowing us to resolve structure across the face of the star on scales as small as 0.1 stellar radii. To explore the effect of limb-darkening on the transit light curve, we divided the available spectral range into 6 subranges (288-400nm; purple, 400-480nm; blue, 480-569nm; green, 569nm-680nm; yellow, 680-800nm; orange, and 800-1022nm; red). A typical spectrum is shown at the bottom left of the poster. Several instrumental effects are prominent, including fringing longward of 750nm, and a break in the continuum between the green and yellow bands, which separate the two gratings (G430L and G750L). For each spectrum, we integrate over each subrange to produce a photometric index, and the resulting time series is divided by a model that accounts for instrumental variations (a linear trend in time, and a polynomial fit in HST-orbital phase), derived from all available out-of-transit data. The 6 resulting time series are shown in the upper panel above.

We then fix the system parameters (i , R_p , R_s) at the best-fit values determined earlier, and find the single-parameter limb-darkening coefficient c_λ [where the normalized stellar surface brightness is described as $B_\lambda(\cos\theta) = 1 - c_\lambda (1 - \cos\theta)$] that minimizes the χ^2 . The best-fit values are (from purple to red) 0.75, 0.67, 0.55, 0.51, 0.41, and 0.33, and the corresponding model light curves are overlotted in the upper panel above. These same curves are replotted in the lower panel above to contrast the differing light curves. As a next step, we won't assume a limb-darkening law, but rather will directly invert the light curves to obtain the stellar surface brightness profile.

Transmission Spectroscopy



Our data will allow us to probe the planetary atmosphere using the technique of transmission spectroscopy. When observed over a bandpass of significant atmospheric opacity, the apparent radius of the planet (as derived from transit measurements) increases, and the transit appears deeper. Using a previous STIS dataset, we used this method to detect sodium absorption. The current dataset has a much greater spectral range, and will allow us to search for additional sources of opacity, notably due to water and Rayleigh scattering. In the figure above, we show theoretical transmission spectra for different model atmospheres. A model with a solar abundance of sodium in atomic form and no clouds is plotted as the dotted line, and is excluded by our previous study, due to its much greater predicted sodium absorption than we observed. Two alternate explanations for the smaller-than-expected sodium signal are a depletion of atomic sodium, or the presence of clouds. Extremes of these models are shown above: The grey curve plots the expected transmission spectrum for a cloudless model with sodium depleted. The solid curve shows a model with a solar abundance of sodium, but with a high cloud deck.

Recently, Vidal-Madjar and colleagues reported the detection of a very deep (15%) absorption at Ly α during times of planetary transit, which they propose is due to a cloud of hydrogen atoms evaporating from the planet. In the figure below, we show the results of our search for the corresponding absorption at H α and H β . We plot the difference in the observed light curve from the adjacent continuum for a bandpass centered on each line. No significant absorption is detected. Note that both time series show a small increase near center of eclipse, and a corresponding decrease during times of ingress and egress (green lines). This effect is due to the reduced limb-darkening in the cores of these lines relative to the adjacent continua.

